Study on the precision of the guide control system of independent wheel

Y ji , L Ren , R Li , W Sun
Institute of Rail Transit, Tongji University, Shanghai 201804, China
E-mail: jiyuanjin@tongji.edu.cn

Abstract. The torque ripple of permanent magnet synchronous motor vector with active control is studied in this paper. The ripple appears because of the impact of position detection and current detection, the error generated in inverter and the influence of motor ontology (magnetic chain harmonic and the cogging effect and so on). Then, the simulation dynamic model of bogie with permanent magnet synchronous motor vector control system is established with MATLAB/Simulink. The stability of bogie with steering control is studied. The relationship between the error of the motor and the precision of the control system is studied. The result shows that the existing motor does not meet the requirements of the control system.

1. Introduction

As low-floor light rail vehicle (LF LRV) as a kind of modern trams becomes an important part of public transportation in large and medium-sized cities of the world. Independently rotating wheel (IRW) is introduced into LF LRV to reduce vehicle floor height effectively. By removing rotational motion constraints of the two wheels, the longitudinal creep forces of wheels are significantly reduced (almost eliminated) and therefore there is no need for the pure rolling action of the wheelset. And the large reduced creep force means that the actuation requires the control. Active control schemes will be much lower. However, there are some disadvantages of the new wheelset configuration. One of the main drawbacks is that the independently rotating wheelset does not own natural curve-passing ability as the conventional wheelset, hence the methods of steering control must be provided. The self-curving and centering effect can be slightly restored by gravitational force if a worn type of wheel profile with a specially designed tread is used [1]. This restoring effect is, however, much less effective than the rolling radius effect of a conventional wheelset and is not large enough to affect behavior on curves [2]. In addition, instability is still observed with independently rotating wheelset and additional effect is required to avoid potential oscillations in practice [3]. The performance can be improved by using the coupling between the two wheels. But the coupling wheelset, such as a magnet powder coupling is much softer than elastically constrained solid-axle wheelset [4]. An unsymmetrical structure where a mixture of solid-axle and independently rotating wheelsets has also been proposed to improve the dynamic stability and the ability of steering on curves [5]. MEI studied a dynamics control system for rail vehicles using independently-driven wheel motors based upon a novel traction motor where the motor is embedded inside a wheel, and studies the dynamic behavior of a rail vehicle equipped with such motors [6].An approach of active steering control, which

based on the feedback of rotating speeds of two wheels on the same axle, is given to improve the steering capability of IRW with hub motors [7] [8].

The wheel hub motor is a direct connection between the rotor of the traction motor and the independent wheel and the stator is embedded in the wheel rim. There is no gear transmission device, which supplies compact structure and saves space. The wheel hub motor can be a DC or an AC motor. With the rapid development of permanent magnet motor technology, synchronous permanent magnet motor and brushless DC motor have been widely used in the electric power assisted vehicle. For the ideal permanent magnet synchronous motor, it supplies the ideal sine wave power. The motor with a sinusoidal distribution of windings and uniform air gap, its torque is constant without fluctuation. In fact, the motor torque will ripple due to the design, manufacturing error, control delay and other reasons [9].

This paper studies the torque ripple of the vector control algorithm of the vehicle mounted permanent magnet synchronous motor. The source of the torque ripple is analyzed. The model of a permanent magnet synchronous motor for estimating motor system error is established. The speed deviation of left and right wheels is the feedback of active steering control of the wheel hub motor independent wheel. The stability of bogie with single wheel with control element is investigated. The relationship between the wheel/rail steering system control precision and motor system error for boundary conditions of control system is analyzed.

2. Error of traction control system

2.1. Analysis of torque ripple of permanent magnet synchronous motor

The PMSMs have been applied in some situations such as machine tools and robotics. Speed control of PMSM usually requires a mechanical sensor for obtaining the position of rotor to as a feedback. The PMSM model in the stationary reference frame ($\alpha\beta$-axis)is shown as follow:

$$\begin{cases} \dot{i_\alpha} = -\frac{R}{L}i_\alpha - \frac{1}{L}e_\alpha + \frac{1}{L}u_\alpha \\ \dot{i_\beta} = -\frac{R}{L}i_\beta - \frac{1}{L}e_\beta + \frac{1}{L}u_\beta \\ e_\alpha = -\lambda_0\omega_e sin\theta_e \\ e_\beta = \lambda_0\omega_e cos\theta_e \end{cases} \tag{1}$$

where R is the stator resistance (ohm), L is stator self inductance (H), i_α,i_β,u_α,$u_\beta$ande_α,$e_\beta$are the phase currents (amp), phase voltages (volt) and back emf (volt) in the stationary reference frame, respectively. The ω_e is electrical angular velocity (rad/sec), λ_0 is the flux linkage of permanent magnet (volt.sec/rad) and θ_e is the electrical rotor position (rad).

igure 1 shows the block diagram of the PMSM vector control system, which consists of a rotating speed outer loop and two current inner loops. There are detections of permanent magnet rotor magnetic pole position and speed, coordinate transformation module, current regulator, PWM module, IGBT and so on. The speed of a given motor is compared with that obtained by the position sensor, and then the signal goes through PI adjuster to be output as the signal for the current controller of the q axis. The sampling three-phase stator current I_A, I_B, I_C are transformed through the CLARKE coordinate into the two-phase stationary alpha beta coordinates of the currenti_α i_β. Then with the PARK transform, the current values of the two phases synchronous rotating d-q coordinate system is obtained, which are I_d, I_q, respectively as the d-axis and q-axis current regulator feedback. Then they are compared with the given value. The deviations are input into the d-axis and q-axis current controller. By adjusting the output reference voltageU_d, U_q, the permanent magnet rotor magnetic pole position information is used to obtain the two-phase stationary alpha beta coordinate system voltageU_α, U_β , through Park inverse transformation. They are transmitted into the space vector modulation module (PWM) module, which outputs the PWM. Then, IGBT is driven to generates three-phase sinusoidal current into the PMSM, which is frequency and amplitude adjustable, Finally, the desired control effect can be achieved.

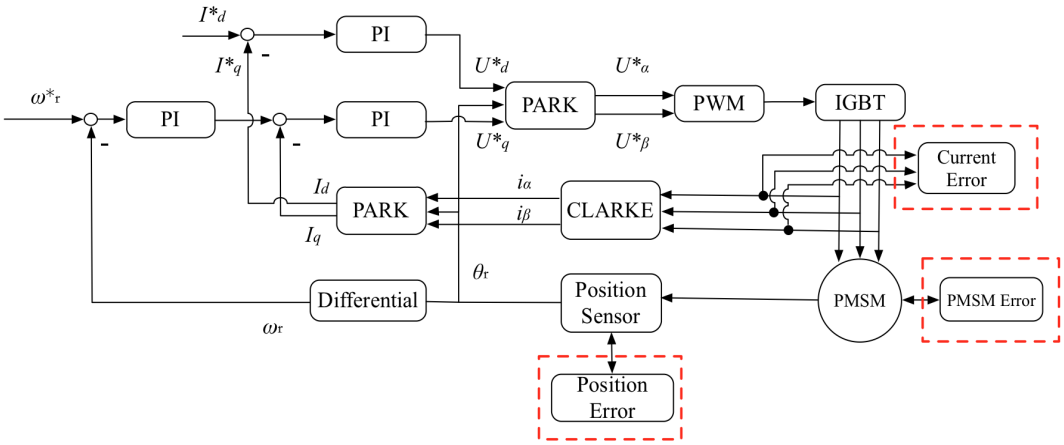

Figure 1. PSMS vector control block diagram

2.2. Error analysis of two-motor synchronization control

One individual independent wheel is usually equipped with one electric motor, and each wheel is driven independently. At present, the synchronous control technology includes parallel control, master slave control, cross coupling control, virtual total axis control, deviation coupling control. In this paper, the deviation coupling control is used. This control strategy was originally proposed by Korne in 1980 [10].. Its control principle diagram is shown in figure 2. The speeds or position signals of the two motors are compared to get a deviation value as the additional feedback signal for cross coupling control strategy. It is the main different characteristic of coupling control strategy from the first control strategy. The additional feedback signal is used as a tracking signal. The system can reflect the change of any motor load, which can obtain good synchronization control precision. The sensor sensitivity is selected to be 0.5% according to the average accuracy of sensors.

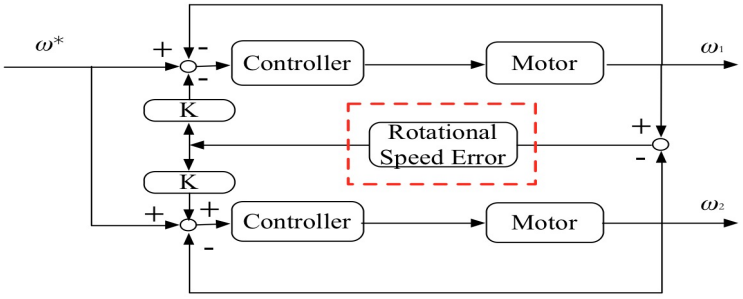

Figure 2. Block diagram of double motor deviation coupling control

2.3. Error simulation analysis of traction control system

According to the above analysis, the control model of the permanent magnet synchronous motor is built in MATLAB/Simulink, and the characteristics of the motor torque fluctuation are investigated. In order to be more similar to the actual working condition, this paper uses the vector control algorithm of the permanent magnet synchronous motor.

In the model, the control mode i_d=0 is adopted, which makes the motor torque control to the control of the current I_q. Vector control simulation model, motor parameter reference for

light rail vehicles 58kw PMSM: the rated motor speed, N_0 =650 $r.min^{-1}$, stator resistance ,R_s =0.08723 Ω, the stator d-axis inductance ,L_D = 0.8 MH, the stator q-axis inductance, L_q= 0.8 MH, rotor flux ,ψ_f= 0.167 WB, number of pole pairs ,p = 22.

The results of dynamic response analysis of PMSM based on vector control principle are shown in Figure 3,4. Results show that: the actual and estimated speeds of the motor can well track the reference value at a constant speed, their deviations are both in range of 8 $r.min^{-}1$ in addition that the startup is large, uniform stage actual speed and speed estimation, ratio maximum of deviation and the rated speed is 0.0122. Because of the existence of motor error, it is necessary to discuss if the precision of independent wheel control system is higher than the error value, when the precision of the motor does not meet the control requirements, the control system does not work.

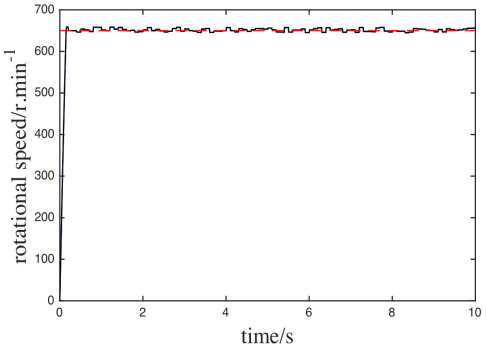

Figure 3. Simulation results of rotor angular velocity of motor

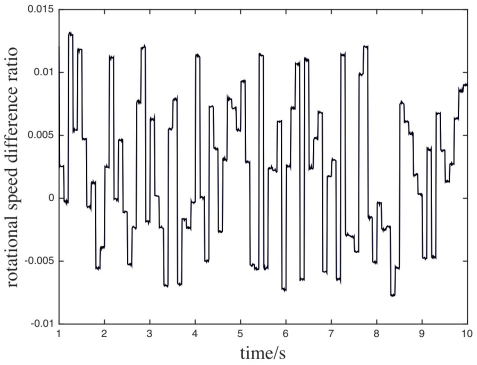

Figure 4. Ratio of motor speed difference and rated speed

3. Stability analysis of bogie with IRW

Each bogie has two independently rotating wheelsets. The wheelsets are connected to the bogie frames with primary suspension system. As the vertical and roll modes have no influence on the steering stability of the bogie, the vertical suspension has not been considered. Figure. 5 shows the half vehicle model. The parameters of the model are given in Table 1. The vehicle model contains eight degrees-of-freedom, i.e. lateral and yaw modes for each wheelset and for the bogie frame, and a lateral mode for the vehicle body (defined by Eqs. (2)-(9)). An actuator is connected between each wheel in the roll direction for the implementation of active control. This actuator can be used for both steering and stability commands.

Table 1. parameter

Symbols	Parameters	Description
M_w	1250 kg	Wheelset mass
I_{wz}	700 kgm^2	Yawing inertia of wheelset
I_{wy}	100 kgm^2	Pitching inertia of wheelset
λ	0.2	conicity
f_{11}	1.5e7	Longitudinal coefficients
f_{22}	1.5e7	lateral coefficients
r	0.46 m	Wheel radius
L_g	0.75 m	Half gauge of wheelset
M_b	2500 kg	Bogie frame mass
k_{py}	5.0e6 N/m	Lateral stiffness of primary suspension
k_{px}	2.0e6 N/m	Longitudinal stiffness of primary suspension
L_t	1.2 m	Half spacing of axles
L_p	0.9 m	Half spacing of primary suspension

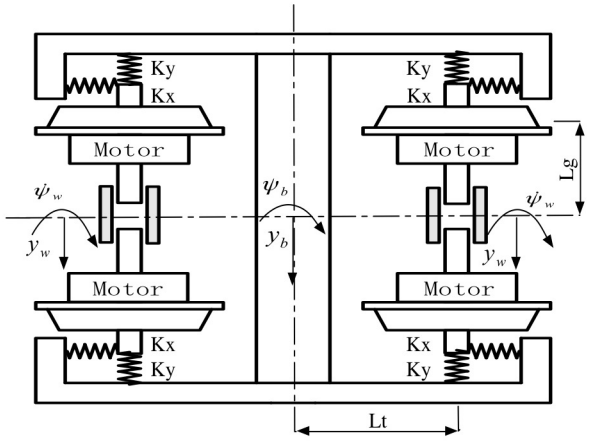

Figure 5. Bogie model with IRW including hub motor

$$m_w\ddot{y}_{w1} + \frac{2f_{22}}{V}\dot{y}_{w1} - 2f_{22}\psi_{w1} + K_y(y_{w1} - y_b - L_t\psi_b) = 0 \tag{2}$$

$$m_w\ddot{y}_{w2} + \frac{2f_{22}}{V}\dot{y}_{w2} - 2f_{22}\psi_{w2} + K_y(y_{w2} - y_b + L_t\psi_b) = 0 \tag{3}$$

$$I_{wz}\ddot{\psi}_{w1} + \frac{2f_{11}L_g\lambda}{r_0}y_{w1} + \frac{2f_{11}L_g^2}{V}\dot{\psi}_{w1} + \frac{2f_{11}L_gr_0}{V}\dot{\phi}_{w1} + K_\psi(\psi_{w1} - \psi_b) = 0 \tag{4}$$

$$I_{wz}\ddot{\psi}_{w2} + \frac{2f_{11}L_g\lambda}{r_0}y_{w2} + \frac{2f_{11}L_g^2}{V}\dot{\psi}_{w2} + \frac{2f_{11}L_gr_0}{V}\dot{\phi}_{w2} + K_\psi(\psi_{w2} - \psi_b) = 0 \tag{5}$$

$$I_{wy}\ddot{\phi}_{w1} + f_{11}\lambda y_{w1} + \frac{f_{11}L_gr_0}{V}\dot{\psi}_{w1} + \frac{f_{11}{r_0}^2}{V}\dot{\phi}_{w1} = T_{\phi1} \tag{6}$$

$$I_{wy}\ddot{\phi}_{w2} + f_{11}\lambda y_{w2} + \frac{f_{11}L_gr_0}{V}\dot{\psi}_{w2} + \frac{f_{11}{r_0}^2}{V}\dot{\phi}_{w2} = T_{\phi2} \tag{7}$$

$$M_b\ddot{y}_b - K_y(y_{w1} - y_b - L_t\psi_b) - K_y(y_{w2} - y_b + L_t\psi_b) = 0 \tag{8}$$

$$I_{wz}\ddot{\psi}_b - K_\psi(\psi_{w1} - \psi_b) - K_\psi(\psi_{w2} - \psi_b) - K_yL_t(y_{w1} - y_b - L_t\psi_b) + K_yL_t(y_{w2} - y_b + L_t\psi_b) = 0 \tag{9}$$

where,$K_\psi = L_g^2 K_x$,$T_{\phi 1} = k\dot{\phi}_{w1}$, $T_{\phi 2} = k\dot{\phi}_{w2}$

The equation (2) - (9) is written in the form of state equation:

$$\dot{x} = A \cdot x + B \cdot u \tag{10}$$

where, X is the state variable, u is the control torque input vector:
$x = [\dot{y}_{w1}, y_{w1}, \dot{\psi}_{w1}, \psi_{w1}, \dot{\phi}_{w1}, \phi_{w1}, \dot{y}_{w2}, y_{w2}, \dot{\psi}_{w2}, \psi_{w2}, \dot{\phi}_{w2}, \phi_{w2}, \dot{y}_b, y_b, \dot{\psi}_b, \psi_b]^T$

$u = [0, 0, 0, 0, T_{\phi 1}, 0, 0, 0, 0, 0, T_{\phi 2}, 0, 0, 0]^T$

In Figure 6, a proportional controller is proposed for the active steering of the wheel hub motor. the proportional gain is less than 102, the proportional gain is very small and the critical speed is constant, which is actually the critical speed of the vehicle; the proportional gain is between 10^2 and 3×10^3, the critical speed is slightly increased, reaching the maximum value near 3×10^3; the proportional gain in between 3×10^3 to 5×10^3, the critical velocity is basically unchanged, the proportional gain greater than 5×10^3 began to decline after, value between 10^4 to 10^5, the critical velocity decreased rapidly, greater than 10^5, the impact of slowing down; the proportional gain is up to 106, the critical speed remains unchanged, then the wheel pair has been tending to the rigid wheel, and the critical speed is close to the value of the rigid wheel. The relationship between the proportional gain and the critical speed provides a reference for further discussion.

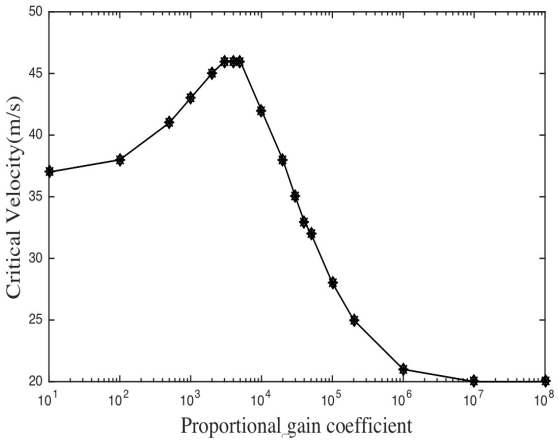

Figure 6. Effect of proportional control gain on critical speed

4. Simulation

Due to the unstable motion of independent wheelset at any speed, the simulation model is the lateral linearization dynamics model of bogie as shown in figure 5, in which only lateral and yaw degrees of freedom are considered. There are eight degrees of freedom in total. According to parameters in table 1, the dynamic model of the bogie is established in Matlab/Simulink with the object oriented dynamic modeling method. The simulation condition is based on figure 6. The proportional gain 10e4 is selected, and the steering frame is 35m/s through long straight line. The steering performance of the wheel is analyzed. When the ratio of the motor speed deviation from the rated speed is less than the error value, the motor error module is introduced and the steering control doesn't work. Otherwise, the control system works. According to the

previous analysis, the error of the motor control system is 0.0122. Figure 7,shows the lateral displacement response of a wheelset excited by a step signal with the initial amplitude 6mm in a horizontal axis under the above simulation conditions. Without control, the lateral maximum displacement of the front steering wheel frame is 114mm. With steering control, the lateral displacement curve of wheelset is the same with no control condition, which indicates that the motor system error is more than the accuracy of control system. And the control system does not work.

It is assumed that the motor control system error value is 0.0122. As figure 8, shows, when the steering control is used, the maximum lateral displacement value of the front wheel frame is not more than 5mm. Therefore, the control system works.

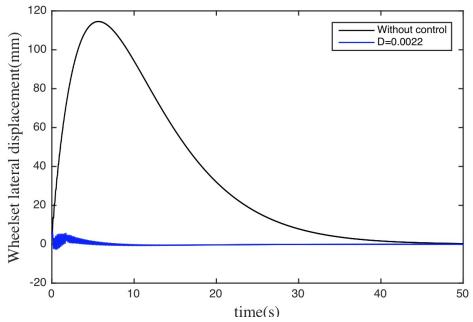

Figure 7. The results of lateral displacement of 6mm

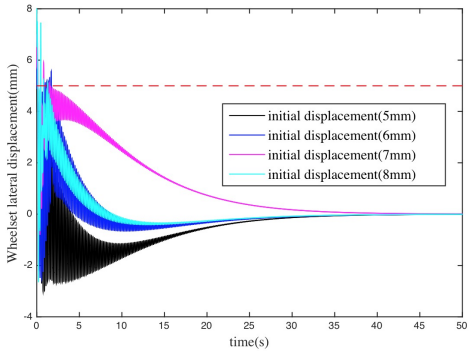

Figure 8. The results of different initial lateral displacement

According to the simulation results of the linear model of bogie, when the wheel/rail contact conicity is 0.2 and the vehicle is passing through the long straight line with the speed of 35m/s, the error of the motor system is greater than that of the control system. Then, the motor cannot meet the requirements of the control system. The bogie is in a free state without any control.

5. Conclusion

In summary, due to the design, manufacturing error, control delay and other factors, the motor torque ripple happens for motor in practice. So the error of the motor system is inevitable. An approach of active steering control, which based on the feedback of rotation speeds of two wheels on the same axle, is given to analyze the steering capability of independently rotating wheelsets(IRW) with hub motors. And the steering ability of the bogie is discussed. The result shows that when the error of the motor system is larger than the precision of the control system, the control system does not work. For now, no better motor exists. So a new or advanced control system should be proposed for this kind of motor to improve the performance of this system. Then the factors that affect the precision of the guide control system of independent wheel will be studied in the future.

6. Acknowledgments

The author(s) disclosed receipt of the following financial support or the research, authorship, and/or publication of this article: The authors acknowledge the financial help provided by the National Science and Technology Support Program of China. (grant no. 2015BAG19B02).

7. References

[1] E. Satou and M. Miyamoto, "Dynamics of a bogie with independently rotating wheels," *Vehicle System Dynamics*, vol. 20, no. sup1, pp. 519–534, 1992.

[2] B. Eickhoff, "The application of independently rotating wheels to railway vehicles," *Proceedings of the Institution of Mechanical Engineers, Part F: Journal of Rail and Rapid Transit*, vol. 205, no. 1, pp. 43–54, 1991.
[3] R. Goodall and H. Li, "Solid axle and independently-rotating railway wheelsets-a control engineering assessment of stability," *Vehicle System Dynamics*, vol. 33, no. 1, pp. 57–67, 2000.
[4] W. Geuenich, C. GÜNTHER, and R. Leo, "The dynamics of fiber composite bogies with creep-controlled wheelsets," *Vehicle System Dynamics*, vol. 12, no. 1-3, pp. 134–140, 1983.
[5] Y. Suda, "Improvement of high speed stability and curving performance by parameter control of trucks for rail vehicles considering independently rotating wheelsets and unsymmetric structure." *JSME international journal. Ser. 3, Vibration, control engineering, engineering for industry*, vol. 33, no. 2, pp. 176–182, 1990.
[6] T. Mei and R. Goodall, "Practical strategies for controlling railway wheelsets independently rotating wheels," *Journal of dynamic systems, measurement, and control*, vol. 125, no. 3, pp. 354–360, 2003.
[7] L. Ren, J. Zhou, and G. Shen, "The active steering control of the independent wheelset with the hub motors," *Zhongguo Tiedao Kexue*, vol. 31, no. 5, pp. 77–83, 2010.
[8] L. REN, J. ZHOU, and G. SHEN, "An approach of active steering of independently rotating wheelsets based on feedback of wheels rotation speed," *China Railway Science*, vol. 1, p. 017, 2006.
[9] X. Li, K. Gutmann, A. Mockel, and C. Kubala, "Permanent magnet synchronous motor torque ripple analysis under ecu caused non-sinusoidal current," in *Future Energy Electronics Conference (IFEEC), 2015 IEEE 2nd International*. IEEE, 2015, pp. 1–6.
[10] Y. Koren, "Cross-coupled biaxial computer control for manufacturing systems," *Journal of Dynamic Systems, Measurement, and Control*, vol. 102, no. 4, pp. 265–272, 1980.